Specific Ion Effects on an Oligopeptide: Bidentate binding matters for the Guanidinium Cation

Vasileios Balos, Bogdan Marekha, Christian Malm, Manfred Wagner, Yuki Nagata, Mischa Bonn and Johannes Hunger*

Specific Ion Effects on an Oligopeptide: Bidentate binding matters for the Guanidinium Cation

Vasileios Balos,[a,b] Bogdan Marekha,[a] Christian Malm,[a] Manfred Wagner,[a] Yuki Nagata,[a] Mischa Bonn[a] and Johannes Hunger*[a]

Abstract: Ion-protein interactions are important for protein function, yet challenging to rationalize due to the multitude of ion-protein interaction possibilities. To explore specific ion effects on protein binding sites, we investigate the interaction of different salts with the zwitterionic peptide triglycine in solution. Dielectric spectroscopy experiments show that salts affect the peptide's reorientational dynamics, with a more pronounced effect of denaturing cations (Li^+, guanidinium Gdm^+) and anions (I^-, SCN^-) than weakly denaturing ones (K^+, Cl^-). Notably, we find the effect of Gdm^+ and Li^+ to be comparable. Molecular dynamics simulations confirm the enhanced binding of Gdm^+ and Li^+ to triglycine, yet with a different binding geometry: While Li^+ predominantly binds to the C-terminal carboxylate group, bidentate binding to the terminus and the nearest amide is particularly important for Gdm^+. This bidentate binding markedly affects peptide conformation. As such, this bidentate binding geometry may help explain the high denaturation activity of Gdm^+ salts.

Specific ion effects, i.e., salts affecting macroscopic properties like surface tension,[1] solubilities,[2,3] interfacial potentials,[4] colloidal stability,[5] and biological activity[5,6] are ubiquitous. Yet, a molecular-level understanding of how ions alter such properties beyond electrostatic effects has not been fully obtained.[7] In particular, understanding how ions affect proteins remains challenging.[6,8,9] Such challenges arise from the structural complexity of proteins and the concomitant broad range of chemically different molecular protein sites.[10]

Model systems such as amide-rich molecules have been often used to elucidate ion-protein interaction.[3,11–18] These amide models, however, lack charged residues (e.g., the C- and N-termini) that are intrinsically sensitive to electrostatic interaction with ions. For small oligopeptides – bearing both an amide backbone and charged moieties – it has been shown that the charged termini play a dominant role for interaction with anions[12] and the presence of the termini has even been suggested to reverse the trends of anion-backbone interaction.[19] Hence, these studies[12,19] have provided – predominantly nuclear magnetic resonance (NMR) spectroscopic and computational – evidence for the termini being crucial when considering the anion-protein interaction. While cation-amide interactions have been shown to be significant,[11,14–16] the effect of cations on oligopeptides and thus the effect of charged termini on interactions of model molecules with cations has been little explored.[20–22]

In the present work, we study the effect of both cations and anions on the oligopeptide triglycine (GGG), which contains both (two) amide groups and charged termini ($-COO^-$ and $-NH_3^+$). To study the relevance of these terminal groups to specific ion effects, we probe the rotational mobility of the zwitterionic triglycine in aqueous solution in the presence of salts. To this end, we use KCl, LiCl, guanidinium chloride (GdmCl), KI and KSCN to study how different anions and cations affect GGG.[23] Comparison to our earlier studies[14,15,17,18] on how these salts affect the rotational mobility of a model amide, *N*-methylacetamide (NMA), and molecular dynamics (MD) simulations on GGG in the presence of KCl, KI, and GdmCl allows us assessing the contribution of the termini on ion-specific interaction strengths.

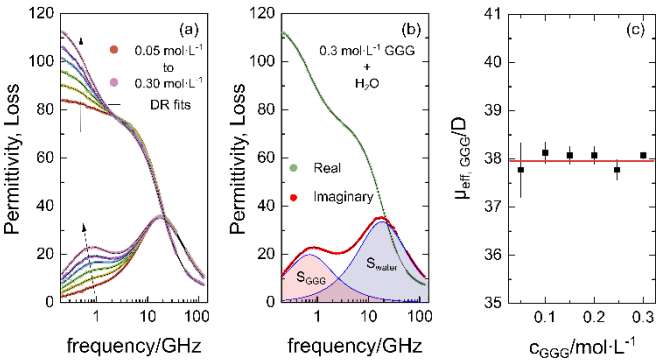

Figure 1. (a) Complex permittivity spectra of aqueous triglycine solutions with c_{GGG} ranging from 0.05 to 0.30 mol·L^{-1} at increments of 0.05 mol·L^{-1}. Arrows indicate increasing GGG concentration. (b) The dielectric spectrum of an aqueous solution of triglycine at c_{GGG} =0.3 mol·L^{-1}. Symbols correspond to experimental data, and solid lines show fits of eq. 1 to the data. Note that the Ohmic loss contribution has been subtracted for visual clarity (last term of eq. 1). The shaded areas show the contribution of the individual relaxation modes (water: shaded blue; GGG: shaded red) to the dielectric loss. (c) Effective dipole moment of triglycine, calculated using eq. S1, as a function of c_{GGG}. The solid red line corresponds to the mean dipole moment, 38 D.

To probe the rotational mobility of GGG in solution, we use dielectric relaxation spectroscopy (DRS).[23,24] This technique records the frequency dependent complex permittivity, $\hat{\varepsilon}(\nu) = \varepsilon'(\nu) - i\varepsilon''(\nu)$, as a measure of the polarization of a sample in an external electric field. For dipolar liquids, the induced polarization at microwave frequencies stems from molecular rotation. For uncorrelated molecular motion, the diffusive rotation of dipolar molecules results in a peak in the dielectric loss (imaginary permittivity, $\varepsilon''(\nu)$) and a dispersion in the dielectric permittivity

[a] Dr. V. Balos, Dr. B. Marekha, Mr. C. Malm, Dr. M. Wagner, Dr. Y. Nagata, Prof. M. Bonn, Dr. J. Hunger
Molecular Spectroscopy Department
Max Planck Institute for Polymer Research
Ackermannweg 10, 55128 Mainz, Germany
E-mail: hunger@mpip-mainz.mpg.de
[b] Present address:
Dr. V. Balos
Department of Physical Chemistry,
Fritz Haber Institute of the Max Planck Society,
Faradayweg 4, 14195 Berlin, Germany

(real permittivity, $\varepsilon'(\nu)$), with the center frequency being characteristic for the rotational relaxation time.

We first characterize the dielectric properties of GGG in aqueous solution. In Fig. 1a we show DRS spectra of aqueous GGG solutions at concentrations ranging from $c_{GGG} = 0.05$ mol·L^{-1} to 0.3 mol·L^{-1}. All spectra in Fig. 1a exhibit a relaxation (peak in $\varepsilon''(\nu)$ and dispersion in $\varepsilon'(\nu)$) at ~ 20 GHz, which can be readily assigned to the relaxation of the hydrogen-bonded water network.[25] Both the center frequency and the relaxation strength (peak amplitude) of this mode are rather insensitive to addition of GGG. Increasing concentration of GGG results in the emergence of a relaxation centered at ~ 1 GHz, indicating that this lower frequency relaxation stems from GGG. This is in line with previous studies of solutions of amino acids.[26,27] The amplitude (dielectric strength) of the emerging GGG relaxation is rather large, as zwitterionic GGG has a large electrical dipole moment and the maximum of the peak in $\varepsilon''(\nu)$ at ~1 GHz shifts to lower frequencies with increasing GGG concentration. This indicates the associated rotational dynamics of GGG is slowed down with increasing c_{GGG}.

To obtain quantitative information from the spectra, we fit a model consisting of two separate relaxations to the experimental data: the water relaxation is modeled using a Cole-Cole relaxation,[28] and the GGG relaxation is modelled using a Debye-type relaxation:[28]

$$\hat{\varepsilon}(\nu) = \frac{S_{GGG}}{1+(2\pi i\nu\tau_{GGG})} + \frac{S_{water}}{1+(2\pi i\nu\tau_{water})^{(1-\alpha_{CC})}} + \varepsilon_\infty + \frac{\kappa}{2\pi i\nu\varepsilon_o} \qquad (1)$$

with S_j and τ_j the relaxation amplitudes and relaxation times, respectively. The Cole-Cole parameter α_{CC} accounts for the symmetric broadening of the water relaxation (compared to a Debye relaxation). ε_∞ is the limiting permittivity at frequencies above the presently studied frequency range. The last term of eq. 1 accounts for Ohmic contributions due to the conductivity of the sample, which we assume to be independent of frequency, i.e. the dc conductivity κ. ε_0 is the permittivity of free space.

This model describes the experimental spectra very well (Fig. 1a). The parameters obtained from fitting the model to the spectra reveal that the relaxation amplitude of water decreases with increasing c_{GGG}, and the decrease can be quantitatively explained by the reduction of the volume concentration of water upon adding GGG (see Supporting Information, SI, Fig. S1). The relaxation time τ_{water} increases continuously from 8.3 ps at $c_{GGG} = 0.0$ mol·L^{-1} (neat water) to 8.7 ps at $c_{GGG} = 0.3$ mol·L^{-1} (Fig. S2, SI). For solutions of amino acids, such slow-down of the average relaxation of water has been related to slower dynamics of a sub-ensemble of water molecules in their hydration shell.[26] Similarly, the relaxation time of GGG, τ_{GGG}, increases from 200 ps at low concentrations to 225 ps at $c_{GGG} = 0.3$ mol·L^{-1}. This increase in relaxation times mirrors the increase in solution viscosity (see Fig. S2a, SI), which suggests that the relaxation is governed by the diffusive rotation of GGG – similar to what has been concluded for amino acids.[26] The relaxation strength, S_{GGG}, increases linearly with increasing c_{GGG} (Fig. S1, SI): As the dielectric relaxation strength scales with the volume concentration of dipoles and the square of their effective electrical dipole moment, this linear scaling indicates that the effective dipole moment does not depend on concentration. Using the Cavell relation,[29] which relates S_{GGG} to c_{GGG} and the effective dipole moment of GGG, $\mu_{eff,GGG}$, ($S_{GGG} \sim c_{GGG} \cdot \mu_{eff,GGG}^2$), we find $\mu_{eff,GGG} \approx 38$ D to be virtually constant over the studied GGG concentration range (Fig. 1c). The insensitivity of $\mu_{eff,GGG}$ to the concentration suggests that – despite the large dipole moment of GGG – the relaxation of GGG is consistent with uncorrelated motion of individual GGG zwitterions.[30]

This notion is in line with findings for zwitterionic glycine, for which dipole correlations have also been found negligible for concentrations up to 2.5 mol·L^{-1}.[26] Hence, our results indicate that the lower frequency dielectric relaxation stems from the rotation of isolated GGG zwitterions in solution and the value of $\mu_{eff,GGG}$ can be related to the average electrical dipole moment of the GGG. Since $\mu_{eff,GGG}$ largely reflects the (average) distance of the charged termini, our experiments provide information on the conformational state of the flexible GGG zwitterion in solution.[20] Indeed, triglycine has been shown to be conformationally rather flexible as the absence of side-chains makes conformational barriers lower as compared to other oligopeptides containing non-Gly residues.[31–33]

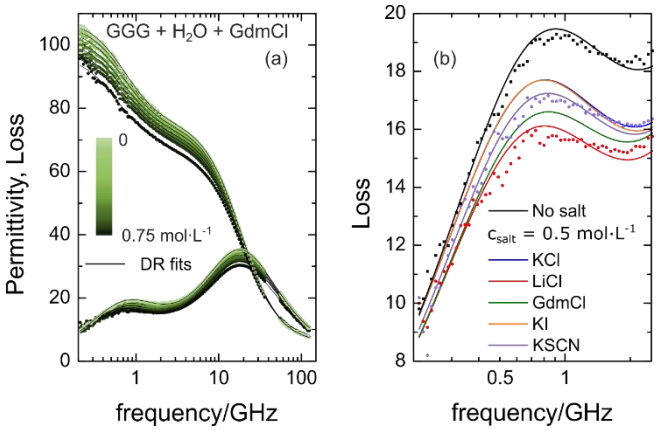

Figure 2. (a) Complex permittivity spectra of 0.25 mol·L^{-1} aqueous solutions of triglycine with increasing concentrations of GdmCl (0, 0.05, 0.10, 0.20, 0.30, 0.40, 0.50, 0.60, 0.75 mol·L^{-1}). The symbols correspond to experimental data and the solid lines show fits using eq. 1. The Ohmic loss contribution (last term of eq. 1) has been subtracted for visual clarity. (b) Zoom into the dielectric loss at low frequencies for 0.25 mol·L^{-1} triglycine solutions with different salts (all 0.50 mol·L^{-1}). Symbols show experimental data for KSCN, LiCl, and in the absence of salt (others omitted for visual clarity) and lines correspond to fits with eq. 1.

As conformational changes are most relevant to the discussion of specific ion-effects below, we explore the contribution of different conformations to $\mu_{eff,GGG}$ with the help of 100 ns long all-atom molecular dynamics (MD) simulations of a dilute GGG solution (for details and contribution of induced dipoles, see SI). The simulations yield a broad dipole moment distribution, peaking around 44 D, with an average value of 40.6±0.3 D (for details see below). This value is in good agreement with the experimentally inferred effective dipole moment of 38.0±0.2 D. The simulations, for which the obtained conformational landscape of GGG is in good agreement with earlier studies (see SI for discussion, Fig. S3), suggest that this value is a population-weighted average of a broad distribution of conformations with a partially stretched

polyglycine II (PGII or 3_1-helix)[21,34] dominating. We also note a small yet statistically significant contribution from conformations with particularly small dipole moments (*ca.* 1.5-2 times smaller than those found for the maximum of the distribution; for details see below). Given that the total dipole moment of GGG originates primarily from the separation of the charged termini, we assign this low-dipole-moment tail of the distribution curve to GGG conformations with C- and N-termini being in close proximity. Our simulations however did not reveal any preferential folding motifs in these low-dipole-moment conformations, in line with the overall flexibility of GGG.

To study the effect of ions on GGG in solution, we probe the dielectric relaxation of GGG in the presence of salts. For these experiments, we vary the concentration of salt c_{salt} = 0 – 0.75 mol·L^{-1} by keeping c_{GGG} = 0.25 mol·L^{-1}. Increasing salt concentration reduces the overall magnitude of the dielectric spectra, as can be seen in Fig. 2a for the addition of GdmCl (for other salts see Fig. S4 of SI). As apparent from the raw data in Fig. 2b, variation of the nature of the salt (at a given salt concentration) results in marked differences in the GGG relaxation, which dominates the spectra at ~1 GHz (see Fig. 1b). Hence, our results show that the interaction of the salts with GGG is ion-specific.

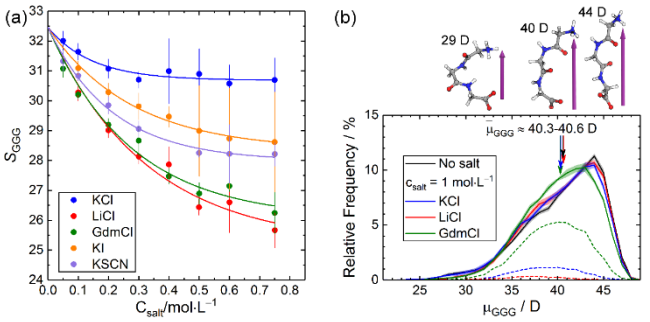

Figure 3. (a) Amplitude (S_{GGG}) of the triglycine relaxation in 0.25 mol·L^{-1} aqueous solutions of triglycine versus salt concentration, as obtained from fitting eq. 1 to the experimental data. The error bars correspond to the standard deviation of six independent measurements. Lines are guide for the eye. (b) Distribution of the dipole moment of GGG obtained from MD simulation of GGG zwitterion in neat water, 1 mol·L^{-1} KCl, 1 mol·L^{-1} LiCl and 1 mol·L^{-1} GdmCl (solid lines). The dipole moment values were obtained using the point charges of the CHARMM C36m force-field and agree well with ab initio calculations, even in the presence of Li^+ and Gdm^+ (see SI). Shaded areas correspond to standard deviations obtained from block-averaging. Vertical arrows indicate the average values. Dashed lines show population-weighted distributions for configurations with GGG simultaneously binding to the same cation via Gly-2 and CTER oxygen atoms. Also shown are representative conformations with low, intermediate, and high dipole moment.

To quantify the ion-specific effects on the GGG reorientational dynamics, we extract the GGG relaxation by fitting eq. 1 to the spectra (Fig. 2a and Figs. S4-S7, SI). For all salts, we find a slow-down of the GGG relaxation (Fig. S6, SI). This increase in τ_{GGG} with increasing c_{salt} is in line with our earlier findings for NMA and can be related to an increase in the samples viscosity with increasing c_{salt}.[14] Conversely, the amplitude of the GGG relaxation S_{GGG} decreases upon addition of salts. While KCl shows a moderate decrease, salts containing anions with a stronger tendency to denature proteins (KI and KSCN) have a more pronounced effect on S_{GGG}. The largest reduction of S_{GGG} is observed for salts where the cations are located at the very edge of the Hofmeister series: LiCl and GdmCl (Fig. 3a). These observed effects for KI, KSCN, and LiCl on GGG are in qualitative agreement with effects reported for these salts interacting with NMA.[14,15,17] For KCl, where the interaction with NMA was found negligible,[14,15,17] we find a minor reduction S_{GGG}. Hence, the interaction of most salts with an isolated amide group in NMA is similar to the interaction with the two amide groups and the termini of GGG. This is not true for GdmCl: while the reduction of the rotational mobility of NMA upon addition of GdmCl was moderate,[14,15,17] we find an enhanced reduction of S_{GGG} due to GdmCl: GdmCl and LiCl affect GGG's rotation to a similar extent. The observed reduction of S_{GGG} – so-called depolarization – is commonly observed for salts dissolved in dipolar liquids and stems from the interaction of the ions with molecular dipoles (e.g., GGG dipoles). Depolarization can have essentially three molecular-level origins: (i) the formation of long-lived ion-dipole contacts can reduce the reorientational relaxation due to irrotational bonding[35] or – similarly - "ion-pairing" with GGG's charged termini.[36,37] A second reason for depolarization, for weaker interactions between dipoles and ions is (ii) the coupling of the translation of the ions to the rotational motion of the dipoles that reduces the amplitudes of the dielectric spectra. Such coupling is referred to as kinetic depolarization (KD):[35,38,39] the dipolar molecules tend to align to the local electric field exerted by a translating ion, rather than the externally applied electric field. Lastly, (iii) a salt-induced reduction of the dipole-moment and/or dipolar correlation can reduce the observed relaxation amplitudes. Long-lived ionic contacts (scenario (i)) between GGG and ions are unlikely: The NMR chemical shifts of the CH_2 groups of GGG, which can evidence such associations from the non-linear variation of the shifts with salt concentration,[19,40] vary nearly linearly with salt concentration (see SI, Fig. S8). A salt-induced reduction of GGG's (scenario (iii)) electrical dipole moment could stem from (de-)protonation of the termini, but this is unlikely, as the effect of salts on the acidity/basicity of the termini is weak.[6] Also altered dipolar correlations seem unlikely, as we find no evidence for such correlations (Fig. 1c). Alternatively, salt-induced changes of the conformational equilibria of the flexible GGG,[31–33] via specific site binding and/or non-specific local charge screening could alter the GGG average dipole moment. Such conformational changes have been, however, suggested to be minor for many monovalent salts.[19,20] Only in the presence of LiCl[21] and SO_3^{2-} anions[20] the conformation of GGG has been suggested to be altered. Here, we find a maximum reduction of S_{GGG} by 21.5 %, which would correspond to a reduction of the average effective dipole moment of GGG by ~10 %.

To explore the relevance of salt-induced conformational changes to GGG to the present experiments, we have extended our MD simulations towards three model systems (for details see SI): one GGG zwitterion in 1 mol·L^{-1} solutions of LiCl, GdmCl, and KCl. The salts induce a slight change in the dipole moment distribution (Fig. 3b). While the simulations reveal subtle salt-specific effects

on the distribution of dipole moments, the MD simulations suggest that the average dipole values are — within error — either the same as for the aqueous solution (LiCl) or only very slightly lower ($\mu_{eff,\ GGG}$ = 40.3±0.3 D for GdmCl and KCl). For GdmCl the insensitivity of the average value, despite the obvious shift of the distribution to lower values, can be traced back to a reduction of the folded conformations (μ_{GGG} < 32 D, Fig. 3b). Hence, a reduction of GGG's dipole (iii) due to conformational changes can also not explain the experimentally observed decrease of S_{GGG}.

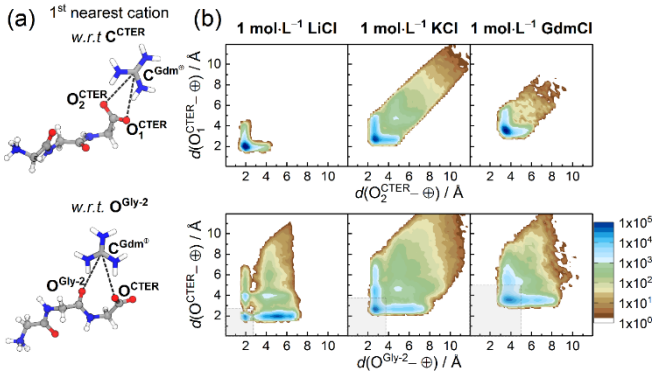

Figure 4. (a) Representative snapshots of the two predominant binding configurations encountered in simulations with GdmCl (CTER stands for C-terminus): Top: simultaneous binding of the cation closest to CTER to both oxygen atoms of the CTER interacting with the two oxygen atoms on the terminal C atom. Bottom: cation closest to Gly-2 residue binding simultaneously to the carbonyl oxygen atom of Gly-2 and to one of the CTER oxygen atoms. The characteristic distances are highlighted with dashed lines. (b) Combined probability distribution functions of the distances between two different oxygen atoms (top: CTER, bottom: Gly-2) of GGG and the central atom of the 1st nearest neighboring cation as obtained from MD simulations in 1 mol·L^{-1} LiCl, KCl and GdmCl solutions. Shaded regions illustrate the combined distance criteria to select the binding configurations for the dipole moment. For their relative occurrence see Fig. 3b.

Hence, kinetic depolarization (scenario (ii)) is the most probable source of the observed decrease in S_{GGG}. As kinetic depolarization requires proximity of the ions to GGG, we study the location of the nearest neighboring cation of GGG as obtained from the MD trajectories. In Fig. 4 we show the combined probability distributions between the center of the cation and two oxygen atoms of GGG for the two oxygen atoms of the C-terminus (top row of Fig. 4) and for the oxygen of the amide next to the C-terminus (bottom row of Fig. 4). Note that for this representation a diagonal probability corresponds to a bidentate interaction of the cation with the oxygens, whereas an elongation along an axis corresponds to a mono-dentate binding configuration.

For the terminal COO^- group the bidentate coordination dominates for all cations, yet with different spatial distributions. Li^+ and Gdm^+ are particularly strongly localized, with a mean distance between the COO^- group and Gdm^+ comparable to that between COO^- groups and arginine residues in proteins (salt bridges,[41] see SI). The similar distance suggests similar binding energies, and points to the mechanism behind protein destabilization. The strong Li^+ and Gdm^+ localization near the COO^- group also explains the observed reduction of the low dipole moment conformations (Fig. 3b), by reducing the electrostatic attraction of the charged termini of GGG. Overall, the proximity of Gdm^+ and Li^+ to the C-terminus of GGG is consistent with the experimentally observed enhanced reduction of S_{GGG} due to KD for GdmCl and LiCl,

The negatively charged COO^- group of GGG is the most obvious binding site for cations, yet the neighboring amide oxygen has also been suggested to be relevant.[42] The combined distributions around the terminal oxygens and the oxygen at Gly-2 are shown in the bottom row of Fig. 4. Similarly to the distribution around the C-terminus, we find both Gdm^+ and Li^+ rather localized, while the nearest K^+ are spread wider. Notably, even though we restrict our analysis to the cations that are closest to the Gly-2 oxygen atom, Li^+ tends to be closer to the terminal oxygen atoms. Conversely, we find the distribution of Gdm^+ and K^+ close to the C-terminus and the Gly-2 oxygen more symmetric. Hence, Gdm^+ (and K^+ to a lesser extent) cations can simultaneously bind to the C-terminal oxygen and the neighboring amide oxygen with a rather high affinity.

To emphasize the high affinity of Gdm^+ to these neighboring oxygen atoms, we calculated the contribution of the conformations of the first peak in the combined distribution (cut-off criteria shown as shaded areas in Fig. 4) to the GGG dipole moments in Fig. 3b (dashed lines). All three distributions are similarly broad and centered around ~39 D, but the contributions of these configurations amount to 48% for GdmCl, while for KCl, and LiCl only to 10.5 % and 2.5 % of all conformation, respectively. Thus, the marked effect of GdmCl on the dipole distribution in Fig. 3b, and also an enhanced kinetic reduction of S_{GGG} for Gdm^+ due to KD can be explained from such coordination.

Altogether, our combined experimental and computational results suggest that salts affect GGG in solution, with subtle effects on the distribution of dipoles. These effects cancel for the mean value of the dipole, which is relevant to the dielectric relaxation amplitudes. The observed salt-specific reduction of the rotational amplitude of GGG dipoles in solutions rather stems from a kinetic effect, with the degree of the reduction being correlated to the probability of the ions to be close to GGG. Our results point toward a different mode of action for Gdm^+ interacting with GGG, as compared to other cations like Li^+, which is consistent with the guanidinium cation not following the general trend of increasing protein denaturation tendency with increasing surface charge density. For the peculiar guanidinium cation, a bidentate binding to the C-terminus and the neighboring amide group is found to be particularly relevant (as opposed to Li^+ and K^+). This bidentate binding is likely related to its ability to form hydrogen-bonds at different, spatially well separated sites[22] (due to the large size of Gdm^+). Thus, despite many electrolyte properties of Gdm^+ salts being rather similar to Na^+ salts,[43–45] and the moderate interaction of GdmCl with amides,[15] this binding motif is probably closely related to its high protein denaturation activity,[46] because it has profound effects on the GGG conformation. We demonstrate the binding here for the C-terminus and the neighboring amide oxygen, it may however be also relevant

across the entire proteins' amide backbone and also to amino acids having carboxylate groups at their side chain. Such carboxylate groups are in fact part of strong intramolecular binding motifs[41] that stabilize the tertiary structure of proteins.

Acknowledgements

This work was funded by the Deutsche Forschungsgemeinschaft (DFG) HU1860/4 and by the European Research Council (ERC) under the European Union's Horizon 2020 research and innovation programme (grant agreement n°714691). B.M. gratefully acknowledges financial support from Alexander von Humboldt Foundation.

Keywords: Hofmeister Effects • Dielectric Spectroscopy • Triglycine • Protein Denaturation • Molecular Dynamics Simulation

[1] M. Manciu, E. Ruckenstein, *Adv. Colloid Interface Sci.* **2003**, *105*, 63–101.
[2] Y. Zhang, S. Furyk, D. E. Bergbreiter, P. S. Cremer, *J. Am. Chem. Soc.* **2005**, *127*, 14505–14510.
[3] E. A. Algaer, N. F. A. van der Vegt, *J. Phys. Chem. B* **2011**, *115*, 13781–13787.
[4] A. M. Jubb, W. Hua, H. C. Allen, *Acc. Chem. Res.* **2012**, *45*, 110–119.
[5] P. Bauduin, A. Renoncourt, D. Touraud, W. Kunz, B. W. Ninham, *Curr. Opin. Colloid Interface Sci.* **2004**, *9*, 43–47.
[6] M. Boström, D. R. M. Williams, B. W. Ninham, *Biophys. J.* **2003**, *85*, 686–694.
[7] A. Salis, B. W. Ninham, *Chem. Soc. Rev.* **2014**, *43*, 7358–7377.
[8] P. Jungwirth, P. S. Cremer, *Nat. Chem.* **2014**, *6*, 261–263.
[9] Y. Zhang, P. S. Cremer, *Proc. Natl. Acad. Sci. U. S. A.* **2009**, *106*, 15249–15253.
[10] H. I. Okur, J. Hladílková, K. B. Rembert, Y. Cho, J. Heyda, J. Dzubiella, P. S. Cremer, P. Jungwirth, *J. Phys. Chem. B* **2017**, *121*, 1997–2014.
[11] H. I. Okur, J. Kherb, P. S. Cremer, *J. Am. Chem. Soc.* **2013**, *135*, 5062–5067.
[12] J. Hladílková, J. Heyda, K. B. Rembert, H. I. Okur, Y. Kurra, W. R. Liu, C. Hilty, P. S. Cremer, P. Jungwirth, *J. Phys. Chem. Lett.* **2013**, *4*, 4069–4073.
[13] H. Kim, H. Lee, G. Lee, H. Kim, M. Cho, *J. Chem. Phys.* **2012**, *136*, 124501.
[14] V. Balos, M. Bonn, J. Hunger, *Phys. Chem. Chem. Phys.* **2015**, *17*, 28539–28543.
[15] V. Balos, H. Kim, M. Bonn, J. Hunger, *Angew. Chemie Int. Ed.* **2016**, *55*, 8125–8128.
[16] C. P. Rao, P. Balaram, C. N. R. Rao, *J. Chem. Soc. Faraday Trans. 1 Phys. Chem. Condens. Phases* **1980**, *76*, 1008–1013.
[17] V. Balos, M. Bonn, J. Hunger, *Phys. Chem. Chem. Phys.* **2016**, *18*, 1346–1347.
[18] V. Balos, M. Bonn, J. Hunger, *Phys. Chem. Chem. Phys.* **2017**, *19*, 9724–9728.
[19] J. Paterová, K. B. Rembert, J. Heyda, Y. Kurra, H. I. Okur, W. R. Liu, C. Hilty, P. S. Cremer, P. Jungwirth, *J. Phys. Chem. B* **2013**, *117*, 8150–8158.
[20] C. P. Schwartz, J. S. Uejio, A. M. Duffin, A. H. England, D. N. Kelly, D. Prendergast, R. J. Saykally, *Proc. Natl. Acad. Sci.* **2010**, *107*, 14008–14013.
[21] S. Bykov, S. Asher, *J. Phys. Chem. B* **2010**, *114*, 6636–6641.
[22] J. Heyda, H. I. Okur, J. Hladílková, K. B. Rembert, W. Hunn, T. Yang, J. Dzubiella, P. Jungwirth, P. S. Cremer, *J. Am. Chem. Soc.* **2017**, *139*, 863–870.
[23] V. Balos, Specific Ion Effects on Protein Fragments - A Dielectric Spectroscopy Study, PhD Thesis, University of Amsterdam, **2017**.
[24] F. Kremer, A. Schönhals, *Broadband Dielectric Spectroscopy*, Springer, Berlin, **2003**.
[25] T. Fukasawa, T. Sato, J. Watanabe, Y. Hama, W. Kunz, R. Buchner, *Phys. Rev. Lett.* **2005**, *95*, 197802.
[26] T. Sato, R. Buchner, Š. Fernandez, A. Chiba, W. Kunz, *J. Mol. Liq.* **2005**, *117*, 93–98.
[27] I. Rodríguez-Arteche, S. Cerveny, Á. Alegría, J. Colmenero, *Phys. Chem. Chem. Phys.* **2012**, *14*, 11352–11362.
[28] C. F. J. Böttcher, *Theory of Electric Polarization*, Elsevier, Amsterdam, **1978**.
[29] E. A. S. Cavell, P. C. Knight, M. A. Sheikh, S. M. A., M. A. Sheikh, *Trans. Faraday Soc.* **1971**, *67*, 2225–2233.
[30] J. Hunger, A. Stoppa, A. Thoman, M. Walther, R. Buchner, *Chem. Phys. Lett.* **2009**, *471*, 85–91.
[31] R. B. Best, X. Zhu, J. Shim, P. E. M. Lopes, J. Mittal, M. Feig, A. D. MacKerell, *J. Chem. Theory Comput.* **2012**, *8*, 3257–3273.
[32] J. A. Drake, B. M. Pettitt, *J. Comput. Chem.* **2015**, *36*, 1275–1285.
[33] J. Graf, P. H. Nguyen, G. Stock, H. Schwalbe, *J. Am. Chem. Soc.* **2007**, *129*, 1179–1189.
[34] R. Schweitzer-Stenner, F. Eker, Q. Huang, K. Griebenow, *J. Am. Chem. Soc.* **2001**, *123*, 9628–9633.
[35] N. Ottosson, J. Hunger, H. J. Bakker, *J. Am. Chem. Soc.* **2014**, *136*, 12808–12811.
[36] A. Eiberweiser, A. Nazet, S. E. Kruchinin, M. V. Fedotova, R. Buchner, *J. Phys. Chem. B* **2015**, *119*, 15203–15211.
[37] S. T. van der Post, J. Hunger, M. Bonn, H. J. Bakker, *J. Phys. Chem. B* **2014**, *118*, 4397–403.
[38] J. B. Hubbard, L. Onsager, W. M. van Beek, M. Mandel, *Proc. Natl. Acad. Sci.* **1977**, *74*, 401–404.
[39] M. Sega, S. Kantorovich, A. Arnold, *Phys. Chem. Chem. Phys.* **2015**, *17*, 130–133.
[40] K. B. Rembert, H. I. Okur, C. Hilty, P. S. Cremer, *Langmuir* **2015**, *31*, 3459–3464.
[41] H. Meuzelaar, M. R. Panman, S. Woutersen, *Angew. Chemie Int. Ed.* **2015**, *54*, 15255–15259.
[42] S. J. Ye, P. B. Armentrout, *J. Phys. Chem. A* **2008**, *112*, 3587–3596.
[43] Y. Marcus, *J. Chem. Thermodyn.* **2012**, *48*, 70–74.
[44] J. Hunger, R. Neueder, R. Buchner, A. Apelblat, *J. Phys. Chem. B* **2013**, *117*, 615–622.
[45] J. Hunger, S. Niedermayer, R. Buchner, G. Hefter, *J. Phys. Chem. B* **2010**, *114*, 13617–13627.
[46] P. H. Von Hippel, K. Y. Wong, *J. Biol. Chem.* **1965**, *240*, 3909–23.